frontiers | Frontiers in Energy Research

ORIGINAL RESEARCH
published: 27 April 2022
doi: 10.3389/fenrg.2022.888107

Day-Ahead Optimal Interval Scheduling for Building Energy System Considering Building Envelope Virtual Energy Storage Uncertainties

Yunfei Mu[1], Yaqing Zhang[1], Zhe Liu[2], Yi Gao[2], Youjun Deng[1], Xiaolong Jin[1], Hongjie Jia[1] and Jiarui Zhang[1]*

[1]Key Laboratory of Smart Grid of Ministry of Education, Tianjin University, Tianjin, China, [2]Global Energy Interconnction Group Co., Ltd., Beijing, China

The heat storage property of building envelopes is usually modeled into virtual energy storage (VES) and regarded as a flexibility resource to support the energy scheduling of building energy systems (BESs). However, the adjustable potential of VES is uncertain, incurred by several ambient random variables with/without specific probability distributions, posing challenges in determining the operational planning schemes of the BES. This article is intended to study a day-ahead optimal scheduling method for a PV-integrated BES (known as PV-BES) with the consideration of VES using interval optimization methods. First, an interval number is used to characterize the uncertainties of outdoor temperature, light irradiance, and the occupant's behavior reflected by the uncontrollable household load. Second, an interval VES model is developed by modeling VES's virtual charge–discharge power (VCDP) with an interval number. Finally, a day-ahead optimal interval scheduling model for the PV-BES considering VES is formulated, aiming to minimize the electricity energy purchase cost of the PV-BES from the external grid. Numerical simulation is conduced, and the results validated the effectiveness of the proposed method.

Keywords: interval optimization, virtual energy storage, building energy system, optimal scheduling, uncertainty

OPEN ACCESS

Edited by:
Shenxi Zhang,
Shanghai Jiao Tong University, China

Reviewed by:
Ke Peng,
Shandong University of Technology, China
Youbo Liu,
Sichuan University, China

****Correspondence:***
Yunfei Mu
yunfeimu@tju.edu.cn

Specialty section:
This article was submitted to Smart Grids, a section of the journal Frontiers in Energy Research

Received: *02 March 2022*
Accepted: *11 March 2022*
Published: *27 April 2022*

Citation:
Mu Y, Zhang Y, Liu Z, Gao Y, Deng Y, Jin X, Jia H and Zhang J (2022) Day-Ahead Optimal Interval Scheduling for Building Energy System Considering Building Envelope Virtual Energy Storage Uncertainties. Front. Energy Res. 10:888107. doi: 10.3389/fenrg.2022.888107

1 INTRODUCTION

With the rapid development of the global economy and the continuous growth of the population, the energy consumption of building heating continues to increase (International Energy Agency, 2020; Pokhrela et al., 2021). In order to reduce carbon emissions in buildings, the introduction of renewable and clean energy in building energy systems (BESs) is being vigorously driven. Due to the advantages of photovoltaic (PV) power generation with easy installation, a short installation period, and no noise, PV has developed rapidly in the BES (Solar Power Europe 2020). Rooftop PV can be combined with buildings and has become a common form for supplying electrical energy (Hong et al., 2014). However, the PV output power has great uncertainty and is difficult to predict. At the same time, the peak-to-valley time of electrical loads of the PV-BES and PV power generation may not be synchronized, which may lead to the problem of the PV local consumption (Rifkin, 2012; Wang et al., 2020).

Some scholars propose to equip the PV-BES with a battery energy storage system (BESS) to realize the reliable local utilization of solar PV generation (Tyagi et al., 2021). However, at present, the installation and maintenance of the BESS is still expensive [e.g., the cost of the BESS is about US$209/kWh in 2020, meaning that the total cost of its installation by considering a BESS with 12 kWh and 2 h duration could reach $5,448 (Deng et al., 2022)], which limits the widespread deployment of the BESS in the end user side (Poonpun and Jewell, 2008; Deng et al., 2021). Due to the thermal inertia of the building envelope, compared with the speed of using electric heating equipment such as air conditioners to increase the indoor temperature, the reduction of the indoor temperature is slower, which makes the building envelope have a certain amount of heat storage capability. To utilize the heat storage capability more efficiently to flexibility for the energy scheduling of the PV-BES, the heat storage capability of the building envelope is usually modeled as a VES model. Without increasing additional investment and space occupation, VES can charge by increasing the electrical power consumption of the air conditioner and the indoor temperature when the PV output power is high or the electricity price is low; VES can discharge by reducing the electrical power consumption of the air conditioner and the indoor temperature when the PV output power is low or the electricity price is high (Oladokun and Odesola, 2015; Ramos et al., 2019; Jin et al., 2020). Therefore, VES can be used as an alternative to the BESS to reduce the electricity energy purchase cost while improving the PV local consumption rate.

In recent years, increasing attention has been drawn on the application of VES for serving the energy scheduling of the BES (Klein et al., 2019; Ji et al., 2020). Considering the relationship between electrical power and heating power of the air conditioner, Zhu et al. (2019) developed a load model of the air conditioner, which regards the variability of air conditioner temperature set points as VES to provide flexibility to the optimal scheduling of the PV-BES. An internal thermal balance model of a building considering the upper and lower boundaries of the indoor temperature comfort range is established by Jin et al. (2017) to introduce VES into the optimal scheduling of the PV-BES. Although the aforementioned studies introduce the concept of VES into the optimal scheduling of the PV-BES, specific parameters (e.g., charge–discharge power and heat storage capacity) are not proposed to quantify the adjustable potential from VES, which will lead to underutilization of VES in the process of serving the energy scheduling for the PV-BES. Nezhad et al. (2020) proposed two quantitative parameters (i.e., the baseline of heating power and the electrical power reduction) to represent the adjustable potential from VES by considering the electrical power used for heating.

Based on the two parameters proposed by Nezhad et al. (2020), Chen et al. (2018) and Liu (2021) proposed a charge–discharge power parameter to quantify the adjustable potential from VES. In addition, Chen et al. (2019), Reynders et al. (2017), and Yang et al. (2019) defined a heat storage capacity parameter of VES by considering the indoor temperature comfort range. Furthermore, with the heat storage capacity parameter, a state of charge parameter is defined by Song et al. (2017) to describe the ratio of the stored electrical energy to the heat storage capacity of VES. However, the influence of the uncertainty of some building energy resource parameters (e.g., outdoor temperature and light irradiance) on VES is ignored in the aforementioned studies, which would cause inaccurate performance quantification of VES and therefore could make the cost-effective operational planning schemes infeasible with the realization of real-time information.

With the consideration of parameter uncertainty, the optimal energy scheduling for the PV-BES essentially becomes an uncertainty optimization problem. Due to the complexity of occupant individual behavior in the building, it is difficult to represent some uncertain parameters with their probability distribution, posing difficulty on the optimal energy scheduling for the PV-BES by using probability distribution-based programming methods, such as stochastic optimization. As one of the main methods for solving uncertainty optimization problems, the interval optimization method can be used to characterize the uncertain factors by an interval number without the known probability distribution (Muncey, 1979; Huang et al., 1995; Stefan and Dorota, 1996). Based on this, the interval optimization method has been applied in many power system uncertainty optimization problems (Wang et al., 2014; Bai et al., 2017; Su et al., 2020). Su et al. (2020) and Bai et al. (2017) used the interval number to characterize the uncertainty of the PV output power and proposed an interval optimization strategy of the PV-BES based on the PV output power interval number. Wang et al. (2014) introduced the interval number of electrical loads, and based on the interval number of electrical loads, Wang et al. (2014) developed a day-ahead optimal scheduling method for the PV-BES.

Based on the earlier discussion, with the aid of the interval optimization method, this study is intended to propose a day-ahead optimal interval scheduling method for the PV-BES by considering the VES uncertainties incurred by several uncertain building energy resource parameters such as indoor/outdoor temperature. The contributions of this study are summarized as follows:

1) Based on the outdoor temperature and light irradiance interval numbers, an interval VES model is developed by modeling its virtual charge–discharge power (VCDP) interval variable, virtual state of charge (VSOC) interval number, and virtual heat storage capacity (VHSC). The proposed interval VES model can quantify the adjustable potential provided by the building envelope while considering the influence of the uncertainties of outdoor temperature and light irradiance.

2) With the aid of the interval optimization theory, an optimal interval scheduling method for the PV-BES with VES utilization is proposed to minimize the electricity energy purchase cost of the PV-BES. The proposed method can realize effective energy cost reduction while improving the local PV consumption in an uncertain ambient environment.

The rest of this article is organized as follows: **Section 2** gives an overview of the system; **Section 3** presents the modeling of building energy resources by using the interval number; **Section 4** presents the proposed day-ahead optimal interval scheduling method for the PV-BES and the solving approach of the proposed model; **Section 5** reports and discusses the simulation study; **Section 6** draws the conclusion and future work.

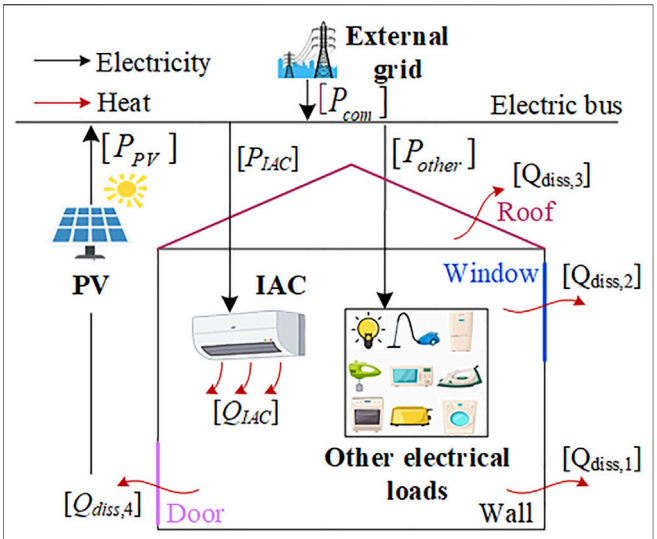

FIGURE 1 | Schematic diagram of the typical PV-BES.

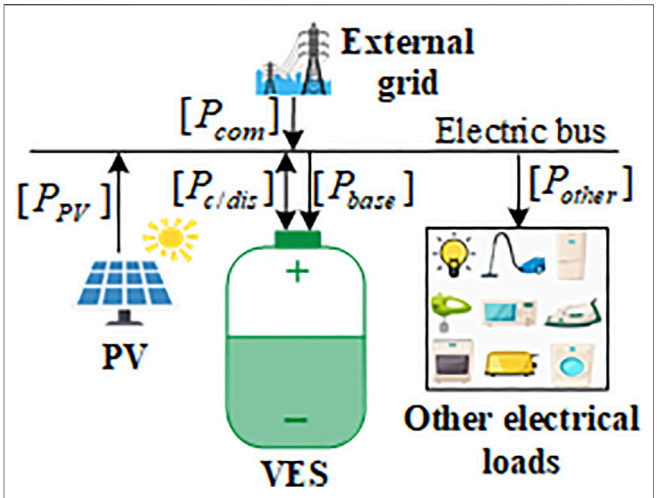

FIGURE 2 | Schematic diagram of the PV-BES with VES.

2 OVERVIEW OF THE PV-BES

A typical grid-connected PV-BES framework is shown in **Figure 1**, mainly consisting of rooftop PV, an inverter air conditioner (IAC), and other electrical loads (OELs), where the OELs are regarded as an uncontrollable household load as a whole. The external grid and rooftop PV provide electrical power to the PV-BES, and the IAC and OELs consume electrical power in the PV-BES, which constitute the electrical power balance of the PV-BES. As an electrothermal conversion device, the IAC can consume electrical power to provide heating power to the PV-BES. The building envelope of the PV-BES dissipates heat. The heat dissipation power of the building envelope and the heating power of the IAC constitute the heating power balance of the PV-BES.

The building envelope and IAC can be modeled as VES shown in **Figure 2** by considering the influence of the uncertainty of outdoor temperature and light irradiance on the adjustable potential that the building envelope can provide to the PV-BES. VES is used to quantify the uncertain adjustable potential provided by the building envelope for optimal scheduling of the PV-BES. When the indoor temperature rises, the building envelope stores heat energy, the VSOC of VES increases, and VES is in a charged state; when the indoor temperature drops, the building envelope releases heat energy, the VSOC of VES decreases, and the VES is in a discharge state. (The definitions of the VSOC and the VCDP are proposed in **Section 3.1.3**.)

3 INTERVAL MODELING FOR BUILDING ENERGY RESOURCES

The interval VES model which is proposed to quantify the adjustable potential of the building envelope, the rooftop PV model based on the interval number, and the OEL model based on the interval number are interval-modeled in this section. For the simplicity and clarification of the modeling expression, the interval numbers that characterize uncertainty are defined as follows:

The symbol " []" is uniformly used to represent interval numbers or interval variables in this article.

$[P_{PV}]$ shown in **Figure 1** is used to describe the PV output power influenced by the uncertainty of light irradiance.

$[P_{PV}] = [P_{PV}^{-}, P_{PV}^{+}]$. In the superscript, "-" indicates the lower limit of the interval number and "+" indicates the upper limit of the interval number.

$[P_{IAC}]$ and $[Q_{IAC}]$ shown in **Figure 1** describe the electrical power P_{IAC} and the heating power Q_{IAC} of IAC. P_{IAC} and Q_{IAC} are uncertain because P_{IAC} and Q_{IAC} are related to the building heating power, which is influenced by outdoor temperature and light irradiance.

$[P_{other}]$ shown in **Figure 1** is defined to describe the OELs influenced by the occupant's behavior.

$[Q_{diss,1}]$~$[Q_{diss,4}]$ shown in **Figure 1** are used to describe the heat dissipation powers corresponding to different building envelopes influenced by the uncertainties of outdoor temperature and light irradiance.

$[P_{com}]$ shown in **Figure 1** represents the commercial power from the external grid and is influenced by $[P_{PV}]$, $[P_{IAC}]$, and $[P_{other}]$. According to the interval number operation rules, $[P_{com}]$ should be defined as an interval number.

$[P_{c/dis}]$ and $[P_{base}]$ shown in **Figure 2** represent the VCDP interval variable and the baseline of the electrical power interval number of the VES, respectively.

3.1 Interval Virtual Energy Storage Model of the Building Envelope

The VES model based on the interval number is developed in this section. First, according to the heat exchange principle of the building envelope, considering the influence of outdoor temperature and light irradiance interval numbers on the heat exchange between the building envelope and indoor air, the interval number of building heat dissipation power is defined. Then, the IAC model is developed to describe the relationship between $P_{IAC}(t)$ and $Q_{IAC}(t)$. Based on the heat dissipation power

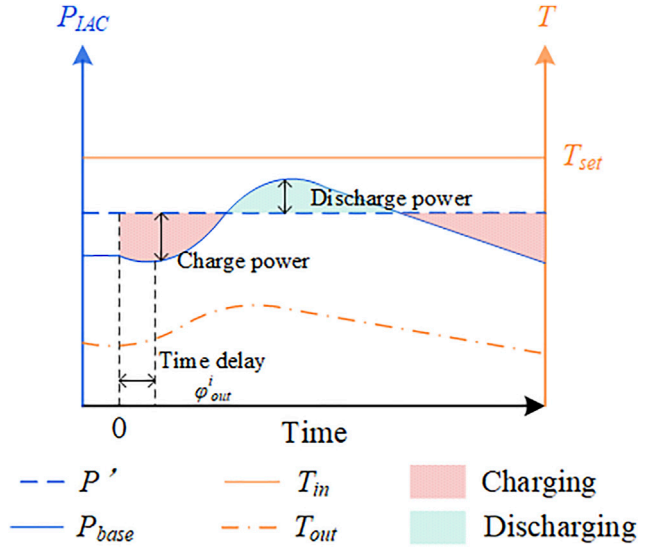

FIGURE 3 | Schematic diagram of the VCDP definition.

and IAC model, a VES model including the VCDP interval variable is developed to realize the interval characterization of the VES.

3.1.1 Building Heat Dissipation Power Based on the Interval Number

As shown in **Figure 1**, when the IAC works at the heating mode, the indoor temperature is higher than the inner surface temperature of the building envelope, which will lead to a heat exchange between the building indoor air and the building envelope (Muncey, 1979). This heat exchange is defined as the heat dissipation power of the building envelope $Q_{diss}(t)$, as shown in **Eq. 1**. $Q_{diss}(t)$ is influenced by outdoor temperature and light irradiance and is defined as the interval number

$$\begin{aligned}[Q_{diss}(t)] &= \sum_{i=1}^{4}[Q_{diss,i}(t)] - [Q_{solar}(t)] \\ &= \sum_{i=1}^{4} F^i \alpha_{in}\left([T_{in}(t)] - [T^i_{sur}(t)]\right) \\ &\quad - [Q_{solar}(t)] 1 \le i \le 4,\ i \in N. \end{aligned} \tag{1}$$

It should be noted that since T_{in} is influenced by the interval variable of the VCDP and $T_{in}(t)$ is also described by the interval number.

$Q_{solar}(t)$ depicted in **Eq. 2** is the heating power contributed by the light radiation through the window to the room at time t, which is related to light irradiance (Muncey, 1979). Therefore, $Q_{solar}(t)$ is defined as the interval number

$$[Q_{solar}(t)] = \lambda_{win} F_{solar} [S_{win}(t)] K_{s,win}, \tag{2}$$

where λ_{win} is the glass transmittance coefficient, F_{solar} is the window area that could project sunlight (m^2), $S_{win}(t)$ is the window light irradiance at time t (kW/m^2), and $K_{s,win}$ is the correction coefficient of the window light irradiance.

$T^i_{sur}(t)$ is influenced by indoor temperature and outdoor temperature and is defined as the interval number shown in **Eq.(3)**

$$[T^i_{sur}(t)] = \left[\bar{T}^i_{sur}\right] + [\Delta T^i_{sur.out}(t)] + [\Delta T^i_{sur.in}(t)]. \tag{3}$$

$\bar{T}^i_{sur}$ is the inner surface daily average temperature of the i-th type building envelope, which is related to the daily average indoor temperature and the daily average outdoor temperature. Therefore, it is defined as the interval number, as shown in **Eq. 4**

$$\left[\bar{T}^i_{sur}\right] = \bar{T}_{in} - \frac{R_{in}}{R^i_0}\left(\bar{T}_{in} - \left[\bar{T}_{out}\right]\right), \tag{4}$$

where $\bar{T}_{out}$ is the daily average outdoor temperature, which is determined by the predicted outdoor temperature (°C). Since the outdoor temperature is the interval number, $\bar{T}_{out}$ should also be expressed by the interval number, and $\bar{T}_{in}$ is the daily average indoor temperature (°C). Since the indoor temperature of the building is usually maintained at T_{set}, $\bar{T}_{in}$ is determined according to the indoor temperature scheme.

$\Delta T^i_{sur.out}(t)$ depicted in **Eq. 5** is the variation in the inner surface temperature of the i-th type building envelope due to the variation of outdoor temperature. $\Delta T^i_{sur.out}(t)$ is related to the variation of outdoor temperature and needed to be defined as the interval number

$$[\Delta T^i_{sur.out}(t)] = \frac{1}{v^i_{out}}\left([T_{out}(t - \varphi^i_{out})] - \left[\bar{T}_{out}\right]\right). \tag{5}$$

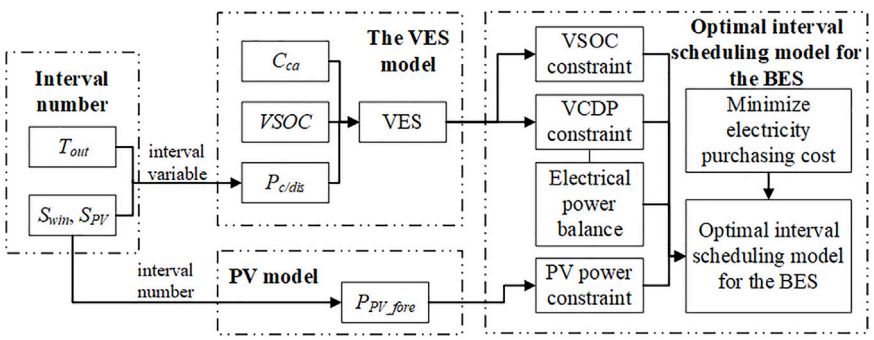

FIGURE 4 | Framework of the day-ahead optimal interval scheduling method based on the interval number.

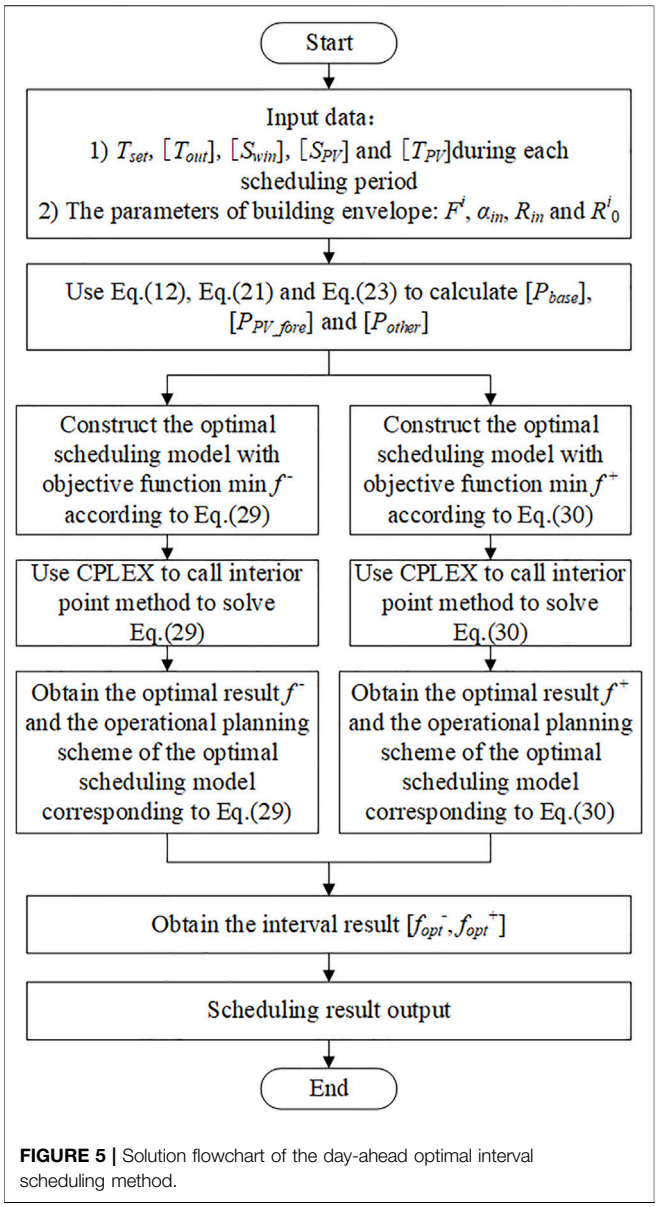

FIGURE 5 | Solution flowchart of the day-ahead optimal interval scheduling method.

$\Delta T^i_{sur.in}(t)$ depicted in **Eq. 6** is the variation in the inner surface temperature of the i-th type building envelope due to the variation of indoor temperature. $\Delta T^i_{sur.in}(t)$ is related to the variation of indoor temperature and needed to be defined as the interval number

$$\left[\Delta T^i_{sur.in}(t)\right] = \frac{1}{v^i_{in}}\left(\left[T_{in}\left(t-\varphi^i_{in}\right)\right] - \bar{T}_{in}\right). \tag{6}$$

v^i_{out}, φ^i_{out}, v^i_{in}, and φ^i_{in} are determined by the materials of the building envelope (Muncey, 1979) (see **Appendix A** for details).

3.1.2 Inverter Air Conditioner Model Based on the Interval Number

According to Kim et al. (2015), the relationship between $P_{IAC}(t)$ and $Q_{IAC}(t)$ can be simplified to the linear relationship depicted in **Eq. 7**. It should be noted that to ensure the occupant's thermal comfort, $P_{IAC}(t)$ and $Q_{IAC}(t)$ are influenced by outdoor temperature and light radiance. Then, $P_{IAC}(t)$ and $Q_{IAC}(t)$ are defined as the interval number.

$$\left[Q_{IAC}(t)\right] = m\left[P_{IAC}(t)\right] + d, \tag{7}$$

where the adjustable range of $P_{IAC}(t)$ is shown in **Eq.(8)**

$$P_{\min} \le \left[P_{IAC}(t)\right] \le P_{\max}. \tag{8}$$

3.1.3 Virtual Energy Storage Model Based on the Interval Number

VES can be regarded as one of the energy storage devices. By analogy to the parameters of energy storage devices (charge–discharge power, capacity, and the state of charge) used in optimal scheduling models (Deng et al., 2021; Deng et al., 2022), the VES model depicted in **Eq. 9** including the VCDP interval variable, VHSC parameter, and VSOC interval number is developed by considering the influence of the uncertainty of outdoor temperature and light irradiance

$$\left[VSOC(k+1)\right] = \frac{\left[VSOC(k)\right]C_{ca} + \left[P_{c/dis}(k)\right]\Delta t}{C_{ca}}. \tag{9}$$

The VCDP is the charge–discharge power of VES, which describes the power variation before and after VES participates in the PV-BES scheduling. The optimal scheduling of the PV-BES is realized by controlling the VCDP. At the same time, because the VCDP is related to the heat dissipation power, the VCDP is defined as an interval variable. The VHSC is the heat capacity of the VES, which describes the maximum heat capacity that VES can provide for the optimal scheduling of the PV-BES. The VSOC is the ratio of the stored electric energy of VES to the VHSC. Since the stored electric energy of VES is related to the VCDP, the VSOC is defined as the interval number.

1) Virtual Charge–Discharge Power

According to Song et al. (2017) and Huang et al. (1995), when $Q_{IAC}(t) = Q_{diss}(t)$, $T_{in} = T_{set}$. Define the heating power that maintains $T_{in} = T_{set}$ as the baseline of the heating power $Q_{base}(t)$. According to **Eq. 1**, $Q_{base}(t)$ is related to the interval numbers $[T^i_{sur}(t)]$ and $[Q_{solar}(t)]$; then, $Q_{base}(t)$ needs to be defined as the interval number, as shown in **Eq. 10**

$$\left[Q_{base}(t)\right] = \sum_{i=1}^{4} F^i \alpha_{in}\left(T_{set} - \left[T^i_{sur}(t)\right]\right) - \left[Q_{solar}(t)\right]. \tag{10}$$

It should be noted that during a specific scheduling period k ($k\Delta t \le t \le (k+1)\Delta t$), the variation of $Q_{base}(t)$ is small and can be regarded as a constant, as shown in **Eq. 11**

$$\left[Q_{base}(k)\right] = \sum_{i=1}^{4} F^i \alpha^i_{in}\left(T_{set} - \left[T^i_{sur}(k)\right]\right) - \left[Q_{solar}(k)\right]. \tag{11}$$

Substituting **Eq. 11** into **Eq. 7**, the baseline of the electrical power corresponding to the baseline of the heating power $Q_{base}(k)$ can be obtained, as shown in **Eq. 12**

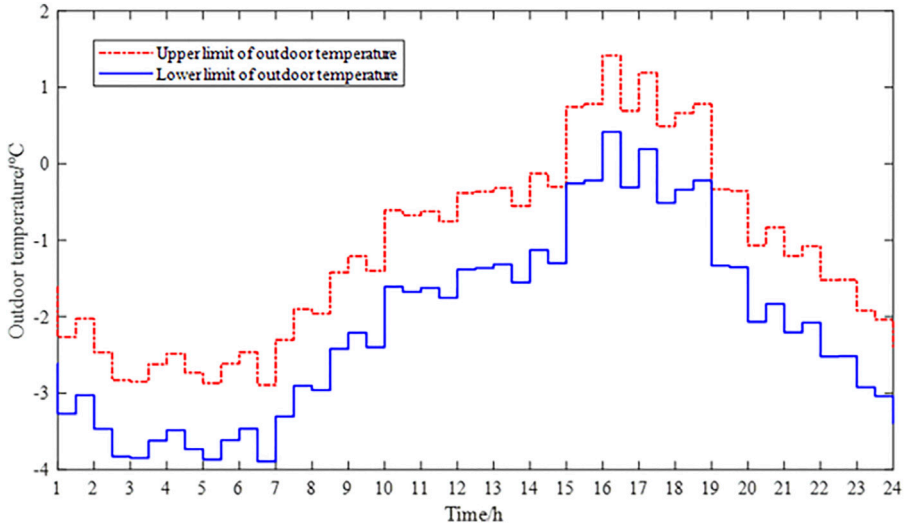

FIGURE 6 | Outdoor temperature prediction interval.

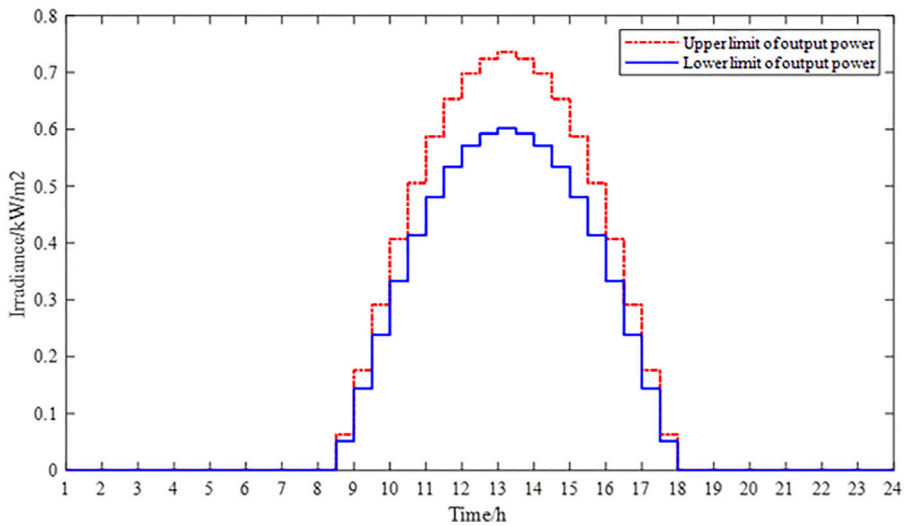

FIGURE 7 | Light irradiance prediction interval.

$$[P_{base}(k)] = \frac{1}{m}\left(\sum_{i=1}^{4} F^i \alpha_{in}^i \left(T_{set} - [T_{sur}^i(k)]\right) - [Q_{solar}(k)]\right) - \frac{d}{m}. \tag{12}$$

As shown in **Figure 3**, when $P_{IAC} = P_{base}$, $T_{in} = T_{set}$. If $P_{IAC} \neq P_{base}$, such as P' shown in **Figure 3**, a power deviation occurs between P_{IAC} and P_{base}, which is defined as the VCDP, as shown in **Eq. 13**. When the VCDP is greater than 0, VES is charged; otherwise, VES is discharged

$$[P_{c/dis}(k)] = \begin{cases} [P_{IAC}(k)] - [P_{base}(k)] > 0, & \text{charging state} \\ [P_{IAC}(k)] - [P_{base}(k)] < 0, & \text{discharging state} \end{cases}. \tag{13}$$

Suppose that $P_{com}(k)$, $P_{PV}(k)$, and $P_{other}(k)$ maintain. Considering the electrical power balance of the PV-BES shown in **Figure 1**, $P_{IAC}(k)$ during the k-th scheduling period is shown in **Eq. 14**

$$[P_{IAC}(k)] = [P_{com}(k)] + [P_{PV}(k)] - [P_{other}(k)]. \tag{14}$$

Substitute **Eq. 14** into **Eq. 13** to obtain **Eq. 15**

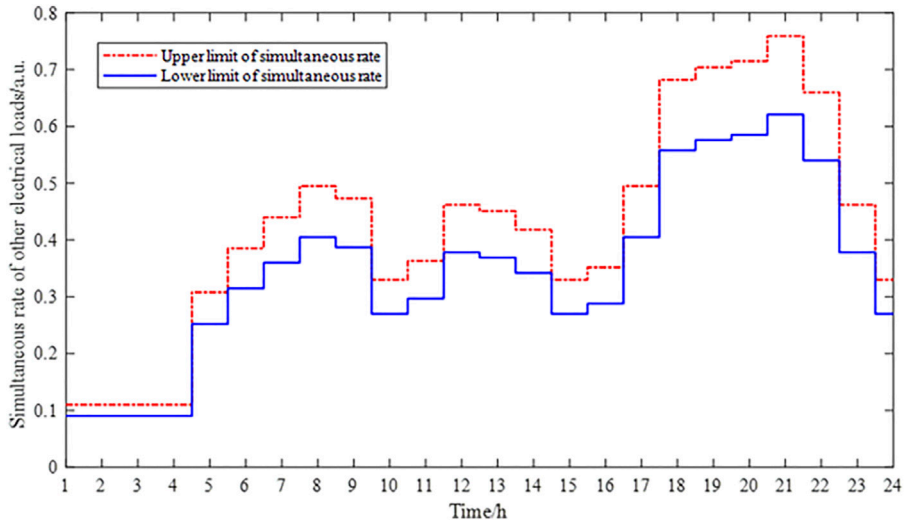

FIGURE 8 | Simultaneous rate prediction interval of OELs.

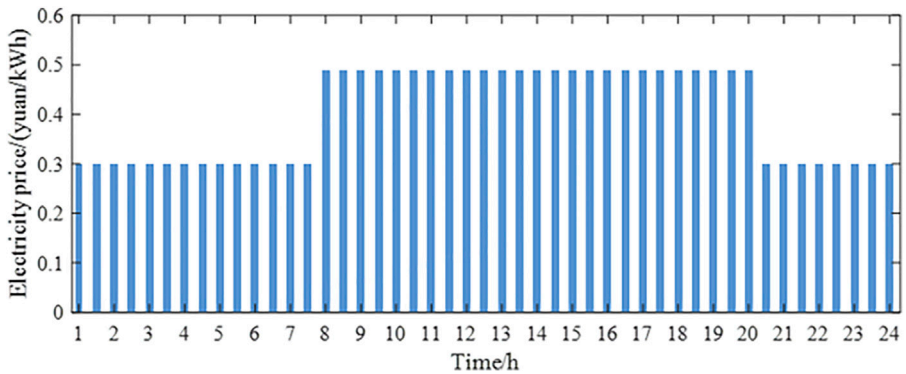

FIGURE 9 | Electricity price.

TABLE 1 | Parameters related to VES and PV.

Parameters	Value	Parameters	Value
F^1	2022.12 m^2	$K_{s,win}$	0.9
F^2	570.24 m^2	T_{PV_ref}	25°C
F^3	530.89 m^2	m	2.00
F^4	9.36 m^2	d	−15.65
α_{in}	8.70 W/m^2°C	P_{min}	0
R_{in}	0.11 m^2°C/W	P_{max}	100 kW
R_0^1	0.60 m^2°C/W	Δt	0.50 h
R_0^2	0.56 m^2°C/W	a	0.0025°C^{-1}
R_0^3	1.53 m^2°C/W	b	0.0005 m^2 / W
R_0^4	2.36 m^2°C/W	c	0.00288°C^{-1}
λ_{win}	67%	P_{PV_max}	100 kW
F_{solar}	570.24 m^2	S_{ref}	1 kW/m^2

$$[P_{c/dis}(k)] = \begin{cases} [P_{com}(k)] + [P_{PV}(k)] - [P_{other}(k)] - [P_{base}(k)] > 0, & \text{charging state} \\ [P_{com}(k)] + [P_{PV}(k)] - [P_{other}(k)] - [P_{base}(k)] < 0, & \text{discharging state} \end{cases} \tag{15}$$

TABLE 2 | Heat lags of building envelopes.

The Type of the building envelope	φ_{out}/h	φ_{in}/h
Wall	10.407 0	0.030 8
Window	0.369 8	0.037 3
Roof	4.109 4	0.034 2
Door	2.747 5	0.003 5

The VCDP is limited by the electrical power range of the IAC as shown in **Eq. 13**, and the maximum discharge power and maximum charge power of VES are shown in **Eqs 16**, **17**. The maximum discharge power $P_{dis\max}(k)$ and the maximum charge power $P_{c\max}(k)$ of VES are both influenced by the interval number $[P_{base}(k)]$. According to the operation rule of the interval number, $P_{dis\max}(k)$ and $P_{c\max}(k)$ should be defined as the number of intervals (Huang et al., 1995)

TABLE 3 | Optimal scheduling results of Scenario I and Scenario II.

	Scenario I (f_{opt}^-)	Scenario I (f_{opt}^+)	Scenario II (f_{opt}^-)	Scenario II (f_{opt}^+)
η/%	88.89	95.78	54.71	61.11
Amounts of purchasing electricity/kWh	1012.68	1052.25	1039.66	1062.27
Electricity energy purchase costs/yuan	365.15	382.53	377.71	389.88

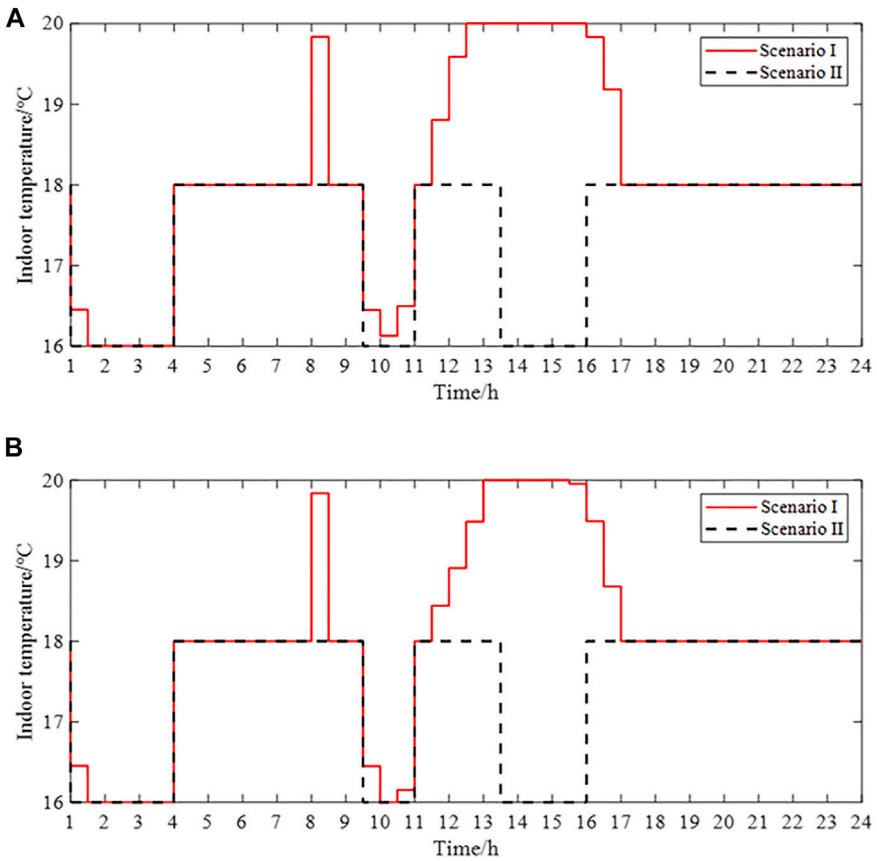

FIGURE 10 | Corresponding indoor temperature when the optimal scheduling results are f_{opt}^- and f_{opt}^+. **(A)** Indoor temperature when the optimal scheduling result is f_{opt}^-. **(B)** Indoor temperature when the optimal scheduling result is f_{opt}^+.

$$[P_{dis\max}(k)] = [P_{base}(k)] - P_{\min} \tag{16}$$

$$[P_{c\max}(k)] = P_{\max} - [P_{base}(k)]. \tag{17}$$

Virtual Heat Storage Capacity

The VHSC is related to the building equivalent heat capacity parameter and the indoor temperature comfort range $[T_{\min}, T_{\max}]$ and is not influenced by outdoor temperature and light radiance. Therefore, the VHSC is defined as a parameter rather than an interval number. According to Song et al. (2017), the VHSC as shown in **Eq. 18**

$$C_{ca} = C(T_{\max} - T_{\min}). \tag{18}$$

Virtual State of Charge

VSOC is defined as the ratio of the stored heat energy of VES to the VHSC, which is used to describe the energy storage state of VES, as shown in **Eq. 19**, and its range is 0–1. When $T_{in} = T_{min}$, VSOC takes 0, and when $T_{in} = T_{max}$, VSOC takes 1

$$[VSOC(k)] = \frac{[E(k)]}{C_{ca}}, \tag{19}$$

$E(k)$ depicted in **Eq. 20** is influenced by T_{in}, and T_{in} will be influenced by the VCDP interval variable. Then, $E(k)$ needs to be defined as the interval number

$$[E(k)] = C([T_{in}(k)] - T_{\min}). \tag{20}$$

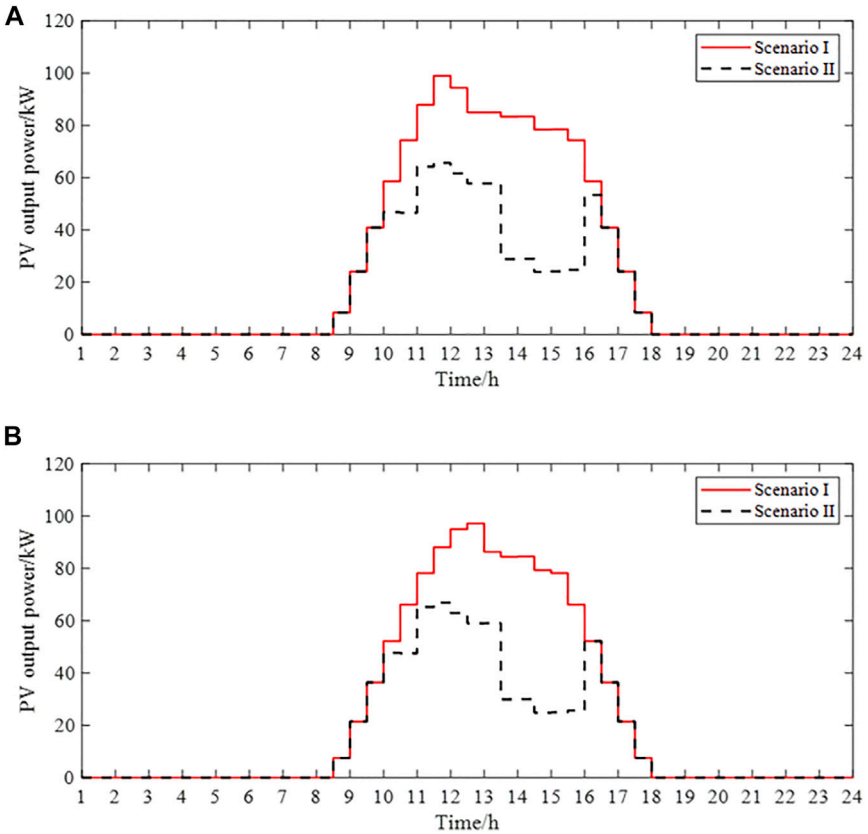

FIGURE 11 | Corresponding PV output power when the optimal scheduling results are f_{opt}^{-} and f_{opt}^{+}. **(A)** PV output power when the optimal scheduling result is f_{opt}^{-}. **(B)** PV output power when the optimal scheduling result is f_{opt}^{+}.

3.2 Rooftop PV Model Based on the Interval Number

Since the PV output power will be influenced by the uncertainty of light irradiance, the rooftop PV model based on the interval number of light irradiance depicted in **Eq. 21** is developed

$$\left[P_{PV\_fore}(k)\right] = P_{PV\_\max} \times \frac{[S_{PV}(k)]}{S_{ref}} \times \left[1 + a\left([T_{PV}(k)] - T_{PV\_ref}\right)\right] \times \ln\left[e + b\left([S_{PV}(k)] - S_{ref}\right)\right] \times \left[1 - c\left([T_{PV}(k)] - T_{PV\_ref}\right)\right]. \tag{21}$$

It is assumed that the PV output power in the PV-BES is only used to meet the power demands of the PV-BES. When the power demand of the PV-BES is smaller than that of the maximum PV output power, the actual PV output power is less than that of the maximum PV output power, which will lead to the problem of the PV local consumption. Therefore, the PV local consumption rate η shown in **Eq. 22** is introduced to describe the PV local consumption of the PV-BES. The larger the η is, the larger the PV local consumption is

$$\eta = \frac{\sum_{k=1}^{48} [P_{PV}(k)]\Delta t}{\sum_{k=1}^{48} \left[P_{PV\_fore}(k)\right]\Delta t}. \tag{22}$$

3.3 Other Electrical Load Models Based on the Interval Number

OELs are generally predicted by the load simultaneous rate (Wang et al., 2014). Due to the uncertainty of the load simultaneous rate, the OEL model depicted in **Eq. 23** is developed by using the interval number of the load simultaneous rate

$$[P_{other}(k)] = [\eta_{other}(k)] \times P_{other.all}, \tag{23}$$

where $\eta_{other}(k)$ is the simultaneous rate of OELs during the k-th scheduling period and $P_{other.all}$ is the sum of the powers of all electrical equipment in the PV-BES except IAC (kW).

4 DAY-AHEAD OPTIMAL INTERVAL SCHEDULING FOR THE PV-BES

Based on the interval optimization theory, a day-ahead optimal interval scheduling method for the PV-BES based on VES is proposed. The method framework is shown in **Figure 4**. Taking the minimum electricity energy purchase cost as the interval objective function and considering the constraints of VES, PV, and the electrical power balance, a day-ahead optimal interval scheduling model considering VES is developed.

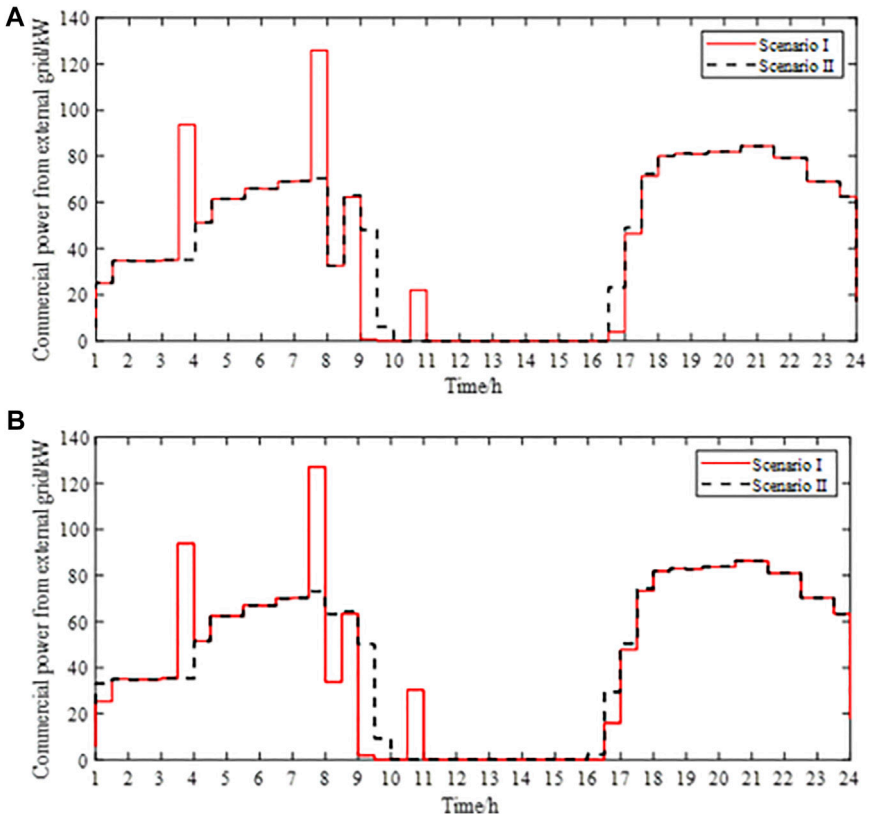

FIGURE 12 | Corresponding commercial power from the external grid when the optimal scheduling results are f_{opt}^{-} and f_{opt}^{+}. **(A)** Commercial power from the external grid when the optimal scheduling result is f_{opt}^{-}. **(B)** Commercial power from the external grid when the optimal scheduling result is f_{opt}^{+}.

4.1 Interval Objective Function

The interval objective function depicted in **Eq. 24** is proposed to minimize the electricity energy purchase cost of the BES. Due to the fact that VES participating in the optimal scheduling of the BES is uncertain, the electricity energy purchase cost is also an interval number (i.e., the objective function is in the form of $[f]$)

$$\min[f] = \sum_{k=1}^{48} ([P_{c/dis}(k)] + [P_{base}(k)] + [P_{other}(k)] - [P_{PV}(k)] \times)\Delta t \times p(k). \tag{24}$$

4.2 Constraints

The optimal interval scheduling model proposed in this article includes VES constraints, the PV output power range constraint, and the electrical power balance constraint, as follows:

1) VES Constraints

(1) VSOC Constraint

The VSOC constraint is used to ensure the occupant's thermal comfort, as shown in **Eq. 25**. When VSOC is 1, T_{in} is equal to T_{max}; when VSOC is 0, T_{in} is equal to T_{min}

$$0 \le [VSOC(k)] \le 1. \tag{25}$$

(2) VCDP Constraint

The VCDP constraint is affected by the maximum charge power and the maximum discharge power of VES, as shown in **Eq. 26**

$$-[P_{dis\max}(k)] \le [P_{c/dis}(k)] \le [P_{c\max}(k)]. \tag{26}$$

2) PV Output Power Range Constraint

The PV output power is constrained by the maximum PV output power, as shown in **Eq. 27**

$$0 \le [P_{PV}(k)] \le \left[P_{PV\_fore}(k)\right]. \tag{27}$$

3) Electrical Power Balance Constraint of the PV-BES

The electrical power balance in the process of PV-BES energy scheduling must be ensured (see **Figure 2**), as shown in constraint **Eq. 28**

$$[P_{com}(k)] + [P_{PV}(k)] = [P_{c/dis}(k)] + [P_{base}(k)] + [P_{other}(k)]. \tag{28}$$

4.3 Model Solving Method

According to the interval optimization theory (Huang et al., 1995), the electricity energy purchase cost interval result of the optimal interval scheduling model shown in **Eqs 24–28** can be obtained by

solving the optimal scheduling models corresponding to the objective function min f^- and min f^+, respectively. The interval result is expressed as $[f_{opt}^-, f_{opt}^+]$. At the same time, the operational planning scheme corresponding to the upper and lower boundaries of the interval result can provide a reference for the formulation of the PV-BES operational planning scheme.

The objective function min f^- and its corresponding constraints are shown in **Eq. 29**

$$\begin{cases} \min\ f^- = \sum_{k=1}^{48} (P_{c/dis}^-(k) + P_{base}^-(k) + P_{other}^-(k) - P_{PV}^-(k))\Delta t \times p(k) \\ 0 \le VSOC(k) \le 1 \\ P_{c/dis}^-(k) \le [P_{c\max}(k)] \\ -P_{c/dis}^+(k) \le [P_{dis\max}(k)] \\ P_{PV}^-(k) \le \left[P_{PV\_fore}(k)\right] \\ P_{PV}^-(k) \ge 0 \\ P_{com}^-(k) + P_{PV}^-(k) - P_{c/dis}^+(k) - P_{base}^+(k) - P_{other}^+(k) \le 0 \\ -P_{com}^+(k) - P_{PV}^+(k) + P_{c/dis}^-(k) + P_{base}^-(k) + P_{other}^-(k) \le 0 \end{cases}, \tag{29}$$

The objective function min f^+ and its corresponding constraints are shown in **Eq.(30)**

$$\begin{cases} \min\ f^+ = \sum_{k=1}^{48} (P+_{c/dis}(k) + P+_{base}(k) + P+_{other}(k) - P+_{PV}(k))\Delta t \times p(k) \\ 0 \le VSOC(k) \le 1 \\ P+_{c/dis}(k) \le [P_{c\max}(k)] \\ -P_{c/dis}^-(k) \le [P_{dis\max}(k)] \\ +_{PV}(k) \le \left[P_{PV\_fore}(k)\right] \\ P+_{PV}(k) \ge 0 \\ P+_{com}(k) + P+_{PV}(k) - P_{c/dis}^-(k) - P_{base}^-(k) - P_{other}^-(k) \le 0 \\ -P-_{com}(k) - P-_{PV}(k) + P+_{c/dis}(k) + P+_{base}(k) + P+_{other}(k) \le 0 \\ P+_{com}(k) \ge P-_{com.opt}(k) \\ P+_{c/dis}(k) \ge P-_{c/dis.opt}(k) \\ P+_{PV}(k) \ge P-_{PV.opt}(k) \\ P+_{base}(k) \ge P-_{base.opt}(k) \\ P+_{other}(k) \ge P-_{other.opt}(k) \end{cases}, \tag{30}$$

Using the CPLEX toolbox and calling the interior point method to solve the two functions shown in **Eqs 29**, **30**, the interval result $[f_{opt}^-, f_{opt}^+]$ of the PV-BES day-ahead optimal interval scheduling model proposed in this article can be obtained. The solution flowchart is shown in **Figure 5**.

5 CASE STUDY

5.1 Input Data and Scenario Setting

A six-story apartment building was used to verify the effectiveness of the day-ahead optimal interval scheduling method based on VES in this study. The effects of four building envelopes, including the wall, window, roof, and door, are considered in this study. Assume that the fluctuation range of the outdoor temperature is ±0.2°C and the fluctuation range of light irradiance and the simultaneous rate of OELs is ±10%. Then, the day-ahead outdoor temperature prediction interval, the light irradiance prediction interval, and the simultaneous rate prediction interval of OELs are shown in **Figures 6–8** (Dong et al., 2020). The electricity price during each scheduling period is shown in **Figure 9** (Tianjin Municipal People's Government, 2020).

Considering the common occupied hours of the building, the indoor temperature scheme is set as follows: during the scheduling period of 4:00–9:00, 11:00–13:00, and 16:00–24:00, the indoor temperature setting value is set to 18°C, and the indoor temperature comfort range is set to 18°C and 20°C; in the remaining time, the indoor temperature setting value is set to 16°C, and the indoor temperature comfort range is set to 16°C and 20°C. The parameters related to the VES and PV are shown in **Table 1**.

According to **Eq. A1** and **Eq. A2** in **Appendix A**, the heat lags of various building envelopes can be obtained, as shown in **Table 2**. Compared with the heat lags when the outdoor temperature is transmitted to the inner surface of the building envelope (φ_{out}), the heat lags when the indoor temperature is transmitted to the inner surface of the building envelope (φ_{in}) are relatively small. Therefore, φ_{in} is ignored to simplify the calculation. The minimum value of φ_{out} in various building envelopes is 0.3698 h, which is about 22 min. Considering that the temperature changes relatively slowly compared with the speed of power energy scheduling and to reduce the solution time of the day-ahead optimal interval scheduling model, the proposed optimal interval scheduling method schedules the PV-BES shown in **Figure 2** over a 24 h time period with a 30 min interval (Δt).

To analyze the effectiveness of the day-ahead optimal interval scheduling method based on the VES proposed in this article, two typical scenarios are set.

Scenario I: Optimal interval scheduling for the PV-BES with the proposed method.

Scenario II: Optimal interval scheduling for the PV-BES without considering VES [following Wang et al. (2014)] (i.e., T_{in} varies with T_{set}).

5.2 Scheduling Results

When the optimal scheduling results are f_{opt}^- and f_{opt}^+, then, the interval results $[f_{opt}^-, f_{opt}^+]$ and the corresponding operational planning schemes for Scenario I and Scenario II are given in this section.

5.2.1 Economic Analysis of Scheduling Results

The interval results (i.e., electricity energy purchase costs) for Scenario I and Scenario II are [365.15, 382.53] and [377.71, 389.88], respectively. When the optimal scheduling results are f_{opt}^- and f_{opt}^+, the corresponding PV local consumption rate, amounts of purchasing electricity, and electricity energy purchase costs for Scenario I and Scenario II are shown in **Table 3**. The variations of indoor temperature, the PV output power, commercial power from the external grid, and the total power consumption of the PV-BES are shown in **Figures 10–13**, respectively.

As shown in **Table 3**, on the basis of ensuring the occupant's thermal comfort (as shown in **Figure 10**), the electricity energy purchase cost is reduced from 377.71 yuan and 389.88 yuan for Scenario II to 365.15 yuan and 382.53 yuan for Scenario I, respectively, a decrease of 3.33 and 1.89%, respectively, and

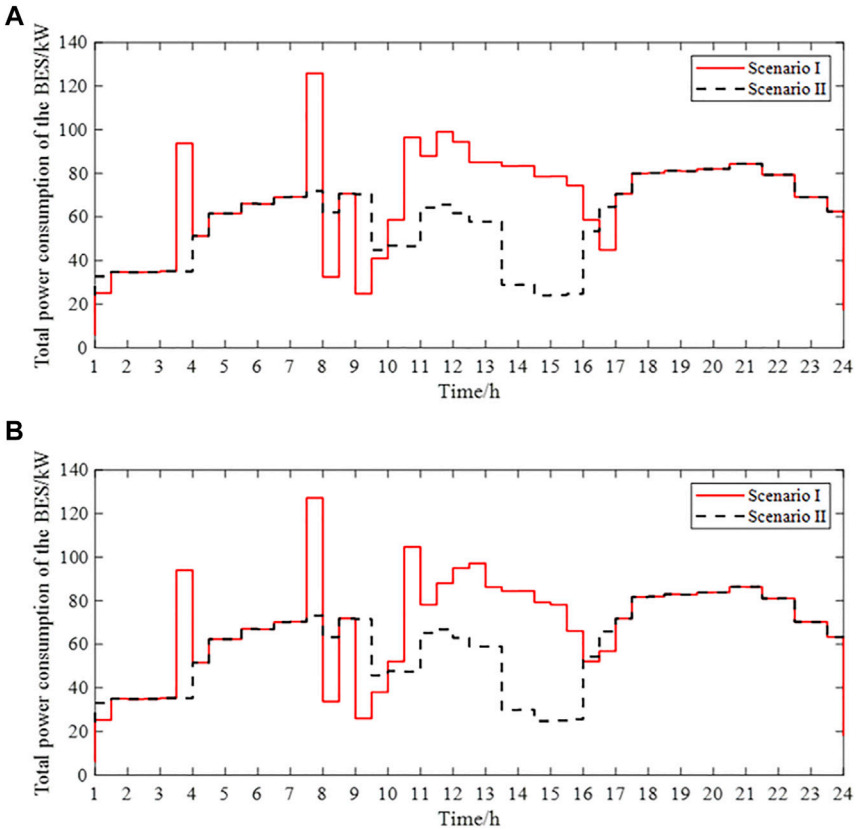

FIGURE 13 | Corresponding total power consumption from the grid when the optimal scheduling results are f_{opt}^- and f_{opt}^+. **(A)** Total power consumption of the BES when the optimal scheduling result is f_{opt}^-. **(B)** Total power consumption of the BES when the optimal scheduling result is f_{opt}^+.

the PV local consumption rate is improved from 54.71 to 61.11% for Scenario II to 88.89 and 95.78% for Scenario I. These data indicate that the day-ahead optimal interval scheduling method based on VES proposed in this article can reduce the electricity energy purchase cost and improve the PV local consumption rate. The reasons are analyzed as follows:

In terms of the economics of the PV-BES: as shown in **Figure 9**, during the scheduling period from 7:30 to 8:00, the electricity price is lower than that in the scheduling periods from 8:00 to 9:30. During the scheduling period from 7:30 to 8:00, compared with the scheduling result without considering VES for Scenario II, the commercial power from the external grid for Scenario I is higher (**Figure 12**). At this time, the VCDP for Scenario I is greater than 0 and the building VES is charged (as shown in **Figures 14**, **15**). During the scheduling periods from 8:00 to 9:30, the electricity price is higher, and the commercial power from the external grid for Scenario I is lower than that for Scenario II, which means that the VCDP for Scenario I is less than 0 and VES releases the charged capacity during the scheduling period from 7:30 to 8:00 (as shown in **Figures 14**, **15**). When the electricity price is high, VES is discharged, and when the electricity price is low, VES is charged, which reduces the electricity energy purchase cost of the PV-BES.

In terms of PV local consumption: VES provided by the building envelope is ignored for Scenario II. The PV local consumption is only achieved by maintaining $T_{in} = T_{set}$ (**Figure 10**) and meeting OELs of the PV-BES (P_{other}). VES is considered for Scenario I, which can provide more flexibility to meet building power demands. During the scheduling periods from 10:00 to 15:30, the maximum PV output power is greater than that in other scheduling periods, and VES for Scenario I is charged (**Figures 10**, **11**). Then, the PV local consumption rate is improved.

In summary, the operational planning scheme with VES based on interval optimization can use VES to reduce the electricity energy purchase cost and improve the PV local consumption rate while considering the uncertainty of outdoor temperature and light irradiance.

5.2.2 Influence of the Uncertainty Degree on the Economics of the PV-BES

To analyze the influence of the uncertainty of outdoor temperature on the economics of the PV-BES, the fluctuation range of outdoor temperature is considered to be ±0.2°C, ±0.5°C, and ±1.0°C. The fluctuation range of light irradiance and the simultaneous rate of OELs is maintained at ±10%. The interval results [f_{opt}^-, f_{opt}^+] corresponding to different fluctuation ranges of outdoor temperature are shown in **Table 4**.

As shown in **Table 4**, with the increase of the uncertainty degree of outdoor temperature, the fluctuation range of the electricity energy purchase cost also increases, which indicates that the uncertainty degree of outdoor temperature has a direct influence on the electricity

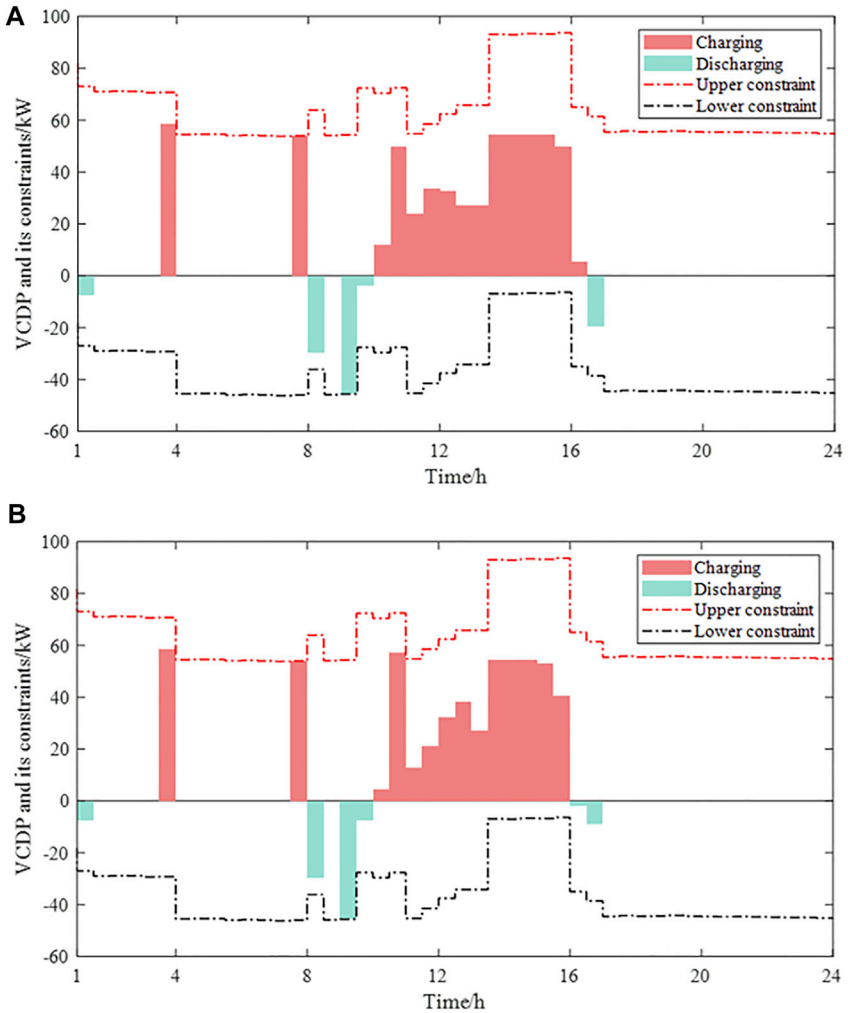

FIGURE 14 | VCDP and its constraints when the optimal scheduling results are f_{opt}^{-} and f_{opt}^{+} for Scenario I. **(A)** VCDP and its constraints when the optimal scheduling result is f_{opt}^{-} for Scenario I. **(B)** VCDP and its constraints when the optimal scheduling result is f_{opt}^{+} for Scenario I.

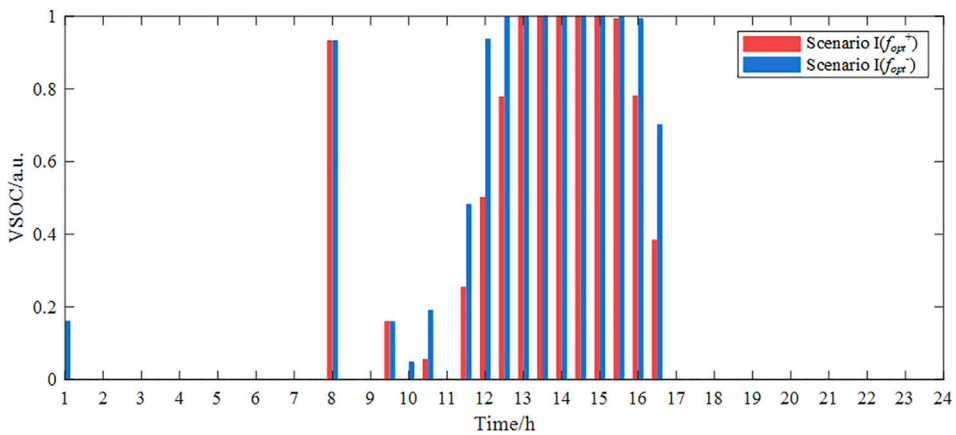

FIGURE 15 | VSOC when the optimal scheduling results are f_{opt}^{-} and f_{opt}^{+} for Scenario I.

energy purchase cost. When the fluctuation range of outdoor temperature is ±0.2°C, the fluctuation range of the electricity energy purchase cost is 17.38 yuan. When the fluctuation range of outdoor temperature increases to ±0.5°C, the fluctuation range of the electricity energy purchase cost increases to 33.55 yuan, and the fluctuation range of the electricity energy purchase cost increases by 93%. When the fluctuation range of outdoor temperature increases to ±1.0°C, the fluctuation range of the electricity energy purchase cost increases to 50.44 yuan. Compared with the outdoor temperature fluctuation range of ±0.2°C, the fluctuation range of the electricity energy purchase cost increases by 190.22%.

To analyze the influence of the uncertainty of light irradiance on the economics of the PV-BES, the fluctuation range of light irradiance is considered to be ±10%, ±15%, and ±20%. The fluctuation range of outdoor temperature is maintained at ±0.2°C, and the simultaneous rate of OELs is maintained at ±10%. The interval results $[f_{opt}^-, f_{opt}^+]$ corresponding to different fluctuation ranges of light irradiance are shown in **Table 5**.

As shown in **Table 5**, with the increase of the uncertainty degree of light irradiance, the fluctuation range of the electricity energy purchase cost also increases, which indicates that the uncertainty degree of light irradiance has a direct influence on the electricity energy purchase cost. When the fluctuation range of light irradiance is ±10%, the fluctuation range of electricity energy purchase cost is 17.38 yuan. When the fluctuation range of light irradiance increases to ±15%, the fluctuation range of the electricity energy purchase cost increases to 43.49 yuan, and the fluctuation range of the electricity energy purchase cost increases by 150.23%. When the fluctuation range of light irradiance increases to ±20%, the fluctuation range of the electricity energy purchase cost increases to 75.24 yuan. Compared with the light irradiance fluctuation range of ±10%, the fluctuation range of the electricity energy purchase cost increases by 332.91%.

TABLE 4 | Electricity energy purchase costs under different outdoor temperature fluctuation ranges.

Fluctuation ranges of the outdoor temperature/°C	(f_{opt}^-, f_{opt}^+)/yuan	Fluctuation ranges of the electricity energy purchase cost/yuan
±0.2	(365.15, 382.53)	17.38
±0.5	(362.39, 395.94)	33.55
±1.0	(354.41, 404.85)	50.44

TABLE 5 | Electricity energy purchase costs under different light irradiance fluctuation ranges.

Fluctuation ranges of the light irradiance/%	(f_{opt}^-, f_{opt}^+)/yuan	Fluctuation ranges of the electricity energy purchase cost/yuan
±10	(365.15, 382.53)	17.38
±15	(364.04, 407.53)	43.49
±20	(360.68, 425.92)	75.24

6 CONCLUSION

In this study, an interval optimization-based day-ahead optimal interval scheduling method for the PV-BES with the consideration of the VES uncertainties is proposed. Particularly, the interval number is used to characterize the uncertain outdoor temperature, light irradiance, and OELs, and then, an interval VES model with VCDP interval variables is proposed. Based on the developed VES model, a cost-effective day-ahead optimal interval scheduling model for the PV-BES is proposed. The conclusions are as follows:

1) The VCDP interval variable and the VSOC interval number are proposed to quantify VES, and a day-ahead optimal interval scheduling method for the PV-BES is proposed by considering the constraints of the adjustable range of the VCDP interval variable and the VSOC interval number. This method can use the VES to participate in the optimal scheduling of the PV-BES while considering the influences of the uncertain outdoor temperature and light irradiance and then reduce the electricity energy purchase cost and improve the PV local consumption rate.
2) The uncertainty of the outdoor temperature and the light irradiance will influence the uncertainty of the PV-BES electricity energy purchase cost. When the fluctuation range of outdoor temperature increases from ±0.2°C to ±1.0°C, the fluctuation range of the PV-BES electricity energy purchase cost increases by 190.22%. When the fluctuation range of light irradiance increases from ±10% to ±20%, the fluctuation range of the PV-BES electricity energy purchase cost increases by 332.91%.
3) In order to further improve the matching degree between the PV-BES operational planning scheme and the actual operating conditions of the PV-BES and improve the operating economics of the PV-BES, future work will focus on developing a multi-time-scale optimal interval scheduling method.

DATA AVAILABILITY STATEMENT

The original contributions presented in the study are included in the article/Supplementary Material, further inquiries can be directed to the corresponding author.

AUTHOR CONTRIBUTIONS

YM, YZ, and JZ conceptualized the study. YZ and YD performed the methodology and were responsible for software. HJ, ZL, and YG validated the results. YZ prepared the original draft. YM, YD, XJ, and JZ reviewed and edited the draft. YM and HJ supervised the study. ZL and YG completed the revised paper.

FUNDING

This paper was funded by the Science and Technology Foundation of Global Energy Interconnection Group Co., Ltd. (No. SGGEIG00JYJS2100033).

REFERENCES

Bai, M., Wang, Y., Tang, W., Wu, C., and Zhang, B. (2017). Day-ahead Optimal Dispatching of Regional Integrated Energy System Based on Interval Linear Programming. *Power Syst. Tech.* 41 (12), 3963–3970. doi:10.13335/j.1000-3673.pst.2017.0390

Chen, X., Wang, J., Xie, J., Xu, S., Yu, K., and Gan, L. (2018). Demand Response Potential Evaluation for Residential Air Conditioning Loads. *IET Generation, Transm. Distribution* 12 (19), 4260–4268. doi:10.1049/iet-gtd.2018.5299

Chen, Y., Chen, Z., Xu, P., Li, W., Sha, H., Yang, Z., et al. (2019). Quantification of Electricity Flexibility in Demand Response: Office Building Case Study. *Energy* 188, 116054. doi:10.1016/j.energy.2019.116054

Deng, Y., Zhang, Y., Luo, F., and Mu, Y. (2021). Operational Planning of Centralized Charging Stations Utilizing Second-Life Battery Energy Storage Systems. *IEEE Trans. Sustain. Energ.* 12 (1), 387–399. doi:10.1109/TSTE.2020.3001015

Deng, Y., Zhang, Y., Luo, F., and Ranzi, G. (2022). Many-Objective HEMS Based on Multi-Scale Occupant Satisfaction Modelling and Second-Life BESS Utilization. *IEEE Trans. Sustain. Energ.* 13, 934–947. doi:10.1109/TSTE.2022.3140765

Dong, J., Li, Y., Zhang, W., Zhang, L., and Lin, Y. (2020). Impact of Residential Building Heating on Natural Gas Consumption in the South of China: Taking Wuhan City as Example. *Energ. Built Environ.* 1 (4), 376–384. doi:10.1016/j.enbenv.2020.04.002

Esmaeel Nezhad, A., Rahimnejad, A., and Gadsden, S. A. (2021). Home Energy Management System for Smart Buildings with Inverter-Based Air Conditioning System. *Int. J. Electr. Power Energ. Syst.* 133, 107230. doi:10.1016/j.ijepes.2021.107230

Hong, T., Koo, C., Park, J., and Park, H. S. (2014). A GIS (Geographic Information System)-Based Optimization Model for Estimating the Electricity Generation of the Rooftop PV (Photovoltaic) System. *Energy* 65, 190–199. doi:10.1016/j.energy.2013.11.082

Huang, G. H., Baetz, B. W., and Patry, G. G. (1995). Grey Fuzzy Integer Programming: An Application to Regional Waste Management Planning under Uncertainty. *Socio-Economic Plann. Sci.* 29 (1), 17–38. doi:10.1016/0377-2217(94)00093-R10.1016/0038-0121(95)98604-t

International Energy Agency (2020). Renewables 2020. AvaliableAt: https://www.iea.org/reports/renewables-2020 (Accessed December 15, 2021).

Ji, Y., Xu, Q., Luan, K., and Yang, B. (2020). Virtual Energy Storage Model of Air Conditioning Loads for Providing Regulation Service. *Energ. Rep.* 6, 627–632. doi:10.1016/j.egyr.2019.11.130

Jin, X., Mu, Y., Jia, H., Wu, J., Jiang, T., and Yu, X. (2017). Dynamic Economic Dispatch of a Hybrid Energy Microgrid Considering Building Based Virtual Energy Storage System. *Appl. Energ.* 194, 386–398. doi:10.1016/j.apenergy.2016.07.080

Jin, X., Qi, F., Wu, Q., Mu, Y., Jia, H., Yu, X., et al. (2020). Integrated Optimal Scheduling and Predictive Control for Energy Management of an Urban Complex Considering Building thermal Dynamics. *Int. J. Electr. Power Energ. Syst.* 123, 106273. doi:10.1016/j.ijepes.2020.106273

Kim, Y.-J., Norford, L. K., and Kirtley, J. L. (2015). Modeling and Analysis of a Variable Speed Heat Pump for Frequency Regulation through Direct Load Control. *IEEE Trans. Power Syst.* 30 (1), 397–408. doi:10.1109/TPWRS.2014.2319310

Klein, K., Herkel, S., Henning, H.-M., and Felsmann, C. (2017). Load Shifting Using the Heating and Cooling System of an Office Building: Quantitative Potential Evaluation for Different Flexibility and Storage Options. *Appl. Energ.* 203, 917–937. doi:10.1016/j.apenergy.2017.06.073

Liu, X. (2021). Multiple Time-scale Economic Dispatching Strategy for Commercial Building with Virtual Energy Storage under Demand Response Mechanism. *Int. J. Energ. Res* 45 (11), 16204–16227. doi:10.1002/er.6853

Muncey, R. (1979). *Heat Transfer Calculations for Buildings*. London: Applied Science Publishers.

Oladokun, M. G., and Odesola, I. A. (2015). Household Energy Consumption and Carbon Emissions for Sustainable Cities - A Critical Review of Modelling Approaches. *Int. J. Sust. Built Environ.* 4 (2), 231–247. doi:10.1016/j.ijsbe.2015.07.005

Pokhrel, S. R., Hewage, K., Chhipi-Shrestha, G., Karunathilake, H., Li, E., and Sadiq, R. (2021). Carbon Capturing for Emissions Reduction at Building Level: A Market Assessment from a Building Management Perspective. *J. Clean. Prod.* 294, 126323. doi:10.1016/j.jclepro.2021.126323

Poonpun, P., and Jewell, W. T. (2008). Analysis of the Cost Per Kilowatt Hour to Store Electricity. *IEEE Trans. Energ. Convers.* 23 (2), 529–534. doi:10.1109/TEC.2007.914157

Reynders, G., Diriken, J., and Saelens, D. (2017). Generic Characterization Method for Energy Flexibility: Applied to Structural thermal Storage in Residential Buildings. *Appl. Energ.* 198, 192–202. doi:10.1016/j.apenergy.2017.04.061

Rifkin, J. (2012). *The Third Industrial Revolution: How Lateral Power is Transforming Energy, the Economy, and the World*. New York, NY: St. Martin's Griffin.

Sánchez Ramos, J., Pavón Moreno, M., Guerrero Delgado, M., Álvarez Domínguez, S., and F. Cabeza, L. (2019). Potential of Energy Flexible Buildings: Evaluation of DSM Strategies Using Building thermal Mass. *Energy and Buildings* 203, 109442. doi:10.1016/j.enbuild.2019.109442

Solar Power Europe (2020). Global Market Outlook 2020-2024. AvaliableAt: https://www.solarpowereurope.org/global-market-outlook-2020-2024/ (Accessed December 15, 2021).

Song, M., Gao, C., Yan, H., and Yang, J. (2018). Thermal Battery Modeling of Inverter Air Conditioning for Demand Response. *IEEE Trans. Smart Grid* 9 (6), 5522–5534. doi:10.1109/TSG.2017.2689820

Stefan, C., and Dorota, K. (1996). Multiobjective Programming in Optimization of Interval Objective Functions - A Generalized Approach. *Eur. J. Oper. Res.* 94 (3), 594–598. doi:10.1016/0377-2217(95)00055-0

Su, Y., Zhou, Y., and Tan, M. (2020). An Interval Optimization Strategy of Household Multi-Energy System Considering Tolerance Degree and Integrated Demand Response. *Appl. Energ.* 260, 114144. doi:10.1016/j.apenergy.2019.114144

Tianjin Municipal People's Government (2020). Subsidies for Clean Heating. AvaliableAt: http://www.tj.gov.cn/ zmhd/hygqx/202006/t20200612_2666059.html (Accessed December 15, 2021).

Tyagi, V. V., Chopra, K., Kalidasan, B., Chauhan, A., Stritih, U., Anand, S., et al. (2021). Phase Change Material Based advance Solar thermal Energy Storage Systems for Building Heating and Cooling Applications: A Prospective Research Approach. *Sustainable Energ. Tech. Assessments* 47, 101318. doi:10.1016/j.seta.2021.101318

Wang, D., Qi, T., Liu, Y., Wang, Y., Fan, J., Wang, Y., et al. (2020). A Method for Evaluating Both Shading and Power Generation Effects of Rooftop Solar PV Panels for Different Climate Zones of China. *Solar Energy* 205, 432–445. doi:10.1016/j.solener.2020.05.009

Wang, S., Wang, D., and Han, L. (2014). Interval Linear Programming Method for Day-Ahead Optimal Economic Dispatching of Microgrid Considering Uncertainty. *Automation Electric Power Syst.* 38 (24), 5–1147. doi:10.7500/AEPS20131212010

Yang, L., Guo, H., Huang, K., and Yang, J. (2019). Optimal Dispatch for a Combined Cooling, Heating and Power Microgrid Considering Building Virtual Energy Storage. *J. Electr. Eng. Technol.* 14 (2), 581–594. doi:10.1007/s42835-018-00055-z

Zhu, X., Yang, J., Liu, Y., Liu, C., Miao, B., and Chen, L. (2019). Optimal Scheduling Method for a Regional Integrated Energy System Considering Joint Virtual Energy Storage. *IEEE Access* 7, 138260–138272. doi:10.1109/ACCESS.2019.2942198

Conflict of Interest: Authors ZL and YG were employed by Global Energy Interconnction Group Co.

The remaining authors declare that the research was conducted in the absence of any commercial or financial relationships that could be construed as a potential conflict of interest.

APPENDIX A

$\varphi_{\frac{i}{out}}$ and $\varphi_{\frac{i}{in}}$ are depicted in **Eq. A1** and **Eq. A2**, respectively (Muncey, 1979)

$$\varphi_{\frac{i}{out}} = 40.5\sum D^i + \arctan\frac{Y_{\frac{i}{out}}}{Y_{\frac{i}{out}} + \alpha_{out}\sqrt{2}} - \arctan\frac{\alpha_{\frac{i}{in}}}{\alpha_{\frac{i}{in}} + Y_{\frac{i}{in}}\sqrt{2}}, \tag{A1}$$

$$\varphi_{\frac{i}{in}} = \arctan\frac{Y_{\frac{i}{in}}}{Y_{\frac{i}{in}} + \alpha_{\frac{i}{in}}\sqrt{2}}, \tag{A2}$$

where m_i is the number of material layers corresponding to the i-th building envelope; D^i is the corresponding thermal inertia index of the i-th type of the building envelope; $Y_{\frac{i}{out}}$ is the heat storage coefficient of the outer surface of the i-th building envelope, W/(m^2°C); and $Y_{\frac{i}{in}}$ is the heat storage coefficient of the inner surface of the i-th building envelope, W/(m^2°C).

$v_{\frac{i}{out}}$ and $v_{\frac{i}{in}}$are depicted in **Eq. A3** and **Eq. A4**, respectively (Muncey, 1979)

$$v_{\frac{i}{out}} = 0.9e^{\frac{\sum D^i}{\sqrt{2}}} \cdot \frac{S_1^i + \alpha_{in}}{S_1^i + Y_{\frac{i}{1.out}}} \cdot \frac{S_2^i + Y_{\frac{i}{1.out}}}{S_2^i + Y_{\frac{i}{2.out}}} \cdots \frac{S_{m_i}^{\frac{i}{}} + Y_{\frac{i}{m_i-1.out}}}{S_{m_i}^{\frac{i}{}} + Y_{\frac{i}{m_i.out}}} \cdot \frac{\alpha_{out} + Y_{\frac{i}{m_i.out}}}{\alpha_{out}} \tag{A3}$$

$$v_{\frac{i}{in}} = 0.95\frac{\alpha_{in} + Y_{\frac{i}{in}}}{\alpha_{in}}. \tag{A4}$$

NOMENCLATURE

VES Virtual energy storage

BES Building energy system

PV Photovoltaic

PV-BES PV-integrated BES

VCDP Virtual charge–discharge power

VHSC Virtual heat storage capacity

VSOC Virtual state of charge

IAC Inverter air conditioner

OELs Other electrical loads

BESS Battery energy storage system

Sets and indices

t Time t (h).

k The k-th scheduling period for a typical day, $1 \le k \le 48$, $k \in N$.

[] Interval number.

Parameters and constants

T_{max} Maximum room temperature (°C).

T_{min} Minimum room temperature (°C).

T_{in} Indoor temperature (°C).

T_{out} Outdoor temperature (°C).

T_{set} Indoor temperature set point determined by the occupant (°C).

$T_{sur}^{i}(t)$ Inner surface temperature of the i-th type building envelope at time t (°C).

λ_{win} Glass transmission coefficient.

P_{min} Minimum input power of IAC (kW).

P_{max} Maximum input power of IAC (kW).

P_{cmax} Maximum charge power of the VES (kW).

P_{dismax} Maximum discharge power of the VES (kW).

C Building equivalent heat capacity parameter (kJ/°C).

F^{i} Inner surface area of i-th type building envelope (m^2).

F_{solar} Window area that can project sunlight (m^2).

α_{in} Heat-transfer coefficient of the inner surface [W/(m^2·°C)].

R_{in} Thermal resistance of the inner surface [(m^2·°C)/W].

R_0^{i} Heat-transfer resistance of the building envelope of the i-th type building envelope [(m^2·°C)/W].

$K_{s,win}$ Window light irradiance correction factor.

v_{out}^{i} Damping factor of the i-th type building envelope for heat transfer from the external surface to the inner surface.

v_{in}^{i} Damping factor of the i-th type building envelope for heat transfer from air to the inner surface.

φ_{out}^{i} Heat lag of the i-th type building envelope from the external surface to inner surface (h).

φ_{in}^{i} Heat lag of the i-th type building envelope from air to the inner surface (h).

C_{ca} The VHSC of VES (kWh).

S_{ref} Standard light irradiance of PV (kW/m^2).

$S_{PV}(k)$ Compensation factor depicting the difference between the actual light irradiance and the standard condition during the k-th scheduling period (kW/m^2).

$S_{win}(t)$ Window light irradiance at time t (kW/m^2).

T_{PV_ref} Standard temperature of PV (kW/m^2).

$T_{PV}(k)$ Compensation factor depicting the difference between the actual temperature of PV and the standard condition during the k-th scheduling period (°C).

m, d Constant coefficients of the IAC.

a, b, c Compensation coefficients of PV

$p(k)$ Electricity price during the k-th scheduling period (yuan/kWh).

P_{PV_max} Maximum PV power under the standard condition (kW).

Variables

$E(k)$ Stored heat energy of VES during the k-th scheduling period (kWh).

$P_{IAC}(t)$ Electrical power of the IAC at time t (kW).

$P_{base}(k)$ Baseline of the electrical power during the k-th scheduling period (kW).

$P_{com}(k)$ Commercial power from the external grid during the k-th scheduling period (kW).

$P_{diss}(t)$ Self-discharge power at time t (kW).

$P_{PV}(k)$ Actual PV power during the k-th scheduling period (kW).

$P_{Pv\_fore}(k)$ Maximum PV power during the k-th scheduling period in a typical day (kW).

$P_{c/dis}(k)$ The VCDP of VES during the k-th scheduling period (kW).

$P_{dismax}(k)$ Maximum discharge power of VES during the k-th scheduling period (kW).

$P_{cmax}(k)$ Maximum charge power of VES during the k-th scheduling period (kW).

$Q_{base}(k)$ Baseline of the heating power during the k-th scheduling period (kW).

$Q_{diss}(t)$ Heat dissipation power at time t (kW).

$Q_{diss,i}(t)$ Heat dissipation power of the i-th type building envelope at time t (kW).

$Q_{IAC}(t)$ Heating power of the IAC at time t (kW).